Asia-Pacific Conference on FRP in Structures (APFIS 2007)
S.T. Smith (ed)

NUMERICAL AND ANALYTICAL INVESTIGATIONS ON IRON COLUMNS REINFORCED BY FRP UNDER AXIAL COMPRESSION

L. LY, J. RONDAL, J.P. JASPART
Division MS²F, Department ArGEnCo, Liège University, Belgium

ABSTRACT

This paper presents numerical and analytical investigations on iron columns under axial compression, strengthened with high modulus carbon fibre reinforced polymer (FRP) sheets. Numerical and analytical models are proposed to predict the resistance and stability load of such elements, including effects of section and member geometrical imperfections and of the nonlinear characteristic and the anisotropy in post elasticity of iron material. It is shown that axial resistance and stiffness of iron columns can be increased significantly with the use of longitudinal FRP sheets as a result of the reduction of the column slenderness, but also that transverse FRP sheets should also be used to avoid any local buckling of the longitudinal FRP sheets during loading.

KEYWORDS

FRP, iron columns, strengthening, numerical investigation, analytical formulation

INTRODUCTION

From the literature, it appears that the behaviour of FRP reinforced metal elements in tension is rather well known, but that little information is available as far as the behaviour of such elements in compression is concerned. Tests on stocky elements with and without FRP are planned to be performed in tension and in compression so as to identify the effect of FRP. In addition, tests on slender columns will also be performed with and without FRP with the objective to identify the influence of FRP on the column stability and resistance. Coupon tests will be also performed to derive the mechanical properties of the constitutive materials of the tested specimens. Once the effect of FRP on iron elements will be determined, the available analytical model for iron columns (Rondal et al. 2003) will be extended to FRP reinforced columns.

In parallel to these experimental activities, a numerical model has been set up. Experimental and numerical investigations are important steps in view of the development and validation of an analytical approach for the prediction of stability and resistance of FRP reinforced iron column under axial compression. In this paper, first numerical and analytical models are presented and preliminary conclusions from the studies are drawn on the beneficial effect of FRP sheets for the resistance and stability of iron columns. The latter are assumed to be circular hollow cast iron elements (figure 1).

Figure 1: Circular hollow cast iron columns

DESIGN SAFETY APPROACH

At the time of using cast iron, the design for structural elements was following an "**allowable stresses**" safety approach based on global safety factor of material strength (values ranging from 4 to 5 for iron in the available literature). Nowadays, another safety approach is proposed and usually used: the **semi-probabilistic approach** based on partial safety factors (safety factors applied on the material strengths and on the actions). For cast iron,

values ranging from 2.16 to 2.7 are proposed for the material safety factors (Käpplein 1991) and a value of about 1.4 for the action safety factors (Eurocode 0). Equivalence between the two methods can be observed as far as elastic design is relevant; indeed, if the material safety factors from the semi-probabilistic approach are multiplied by the action safety factors, that gives values ranging from 3.1 to 3.89 that are close to global safety factors used in the allowable stresses approach. It means that there is no significant difference between both approaches. In this paper, the analytical procedure proposed for the resistance and stability of FRP reinforced iron columns is based on the **semi-probabilistic approach,** used in most recent normative documents such as Eurocode 3.

FRP REINFORCEMENT

Through the performed numerical works which are not detailed in the present paper, the problems of local transfer of shear stresses between FRP and iron elements, especially at the extremities of the FRP strips has been carefully studied. Both cases where compression and tension forces are respectively applied have been investigated. At some distance from the extremities, no relative displacement between FRP and iron is reported and so, in these zones, a full composite interaction between both components may be assumed. Besides that, when compression is applied, a debonding of the FRP strips may be observed which leads to a sort of buckling of the FRP reinforcement and so to a local reduction of section resistance. For sure this last aspect can not be disregarded.

As a result, for FRP material, compressive strains should be limited to prevent such a complex failure mode involving localized debonding associated with local buckling and crushing (Shaat et al. 2007). According to the latter, the limit strain value is equal to 0.13% for steel columns strengthened by high modulus composite materials. That significantly restricts the enhancement of the stiffness and resistance properties of iron columns with FRP whatever the quality of the latter. Therefore, transverse FRP strips should be also applied in addition with longitudinal ones so as to improve the limit compressive strains.

IRON MATERIAL

The mechanical properties of the iron material are highly dependent on the origin and the production period. They are also linked to the type of iron (cast or wrought iron). Values of the ultimate stress $\sigma_{i,u,c}$ ($\sigma_{i,u,t}$) in compression (in tension) can be found from literature, but few information relatives to the full stress-strain behaviour. Normally, iron material exhibits some ductility in compression, but is very brittle in tension. The ratio of the two ultimate strengths ($\sigma_{i,u,t}/\sigma_{i,u,c}$) may range from 0.1 to 0.2.

Nominal values (the 0.2% proof stress $\sigma_{i,0.2}$), considered as the equivalent yield stress, have to be defined. For cast iron, $\sigma_{ι,0.2}$ ($\sigma_{ι,0.2c}$ or $\sigma_{ι,0.2,t}$) in compression or in tension is approximately equal to a half of the ultimate one. Besides that, the $\sigma-\varepsilon$ curve may be approximated through a Ramberg-Osgood one (Rondal et al. 2003):

$$\varepsilon = \frac{\sigma}{E_i} + 0.002\left(\frac{\sigma}{\sigma_{i,0.2}}\right)^n \qquad (1)$$

Here the Ramberg-Osgood parameters (E_i, $\sigma_{ι,0.2}$, n) are assumed to be known. In this paper, E_i = 88000 N/mm², n = 6, $\sigma_{ι,0.2,c}$ = 375 N/mm² and $\sigma_{ι,0.2,t}$ = 75 N/mm². Especially in tension, iron should be limited in its elastic behaviour. Therefore elastic analysis is used to design iron elements, even reinforced by FRP. The 0.2% proof stress ($\sigma_{ι,0.2,c}$ in compression and $\sigma_{ι,0.2,t}$ in tension) will be used as the yield value for the estimation of the "elastic" resistance of iron elements.

FRP MATERIAL

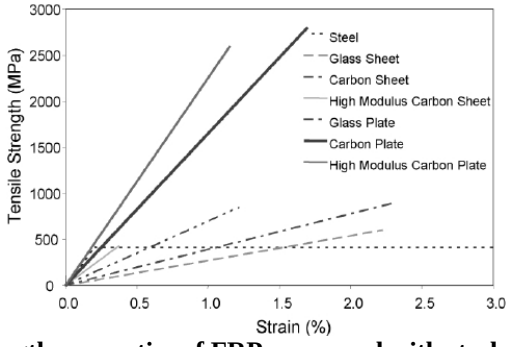

Figure 2: Elastic and strength properties of FRP compared with steel material (Buyukozturk 2004)

The strengthening of steel members with FRP is both mechanically and economically appreciated in retrofitting due to the ease of installation and the potential of eliminating welded and bolted repairs. For structural iron elements in historical buildings, not to change the look of all structure is also a main objective. Applicability and effectiveness of strengthening with FRP depend largely on the material and the type of member to be reinforced. In general, the strengthening material should have a similar or higher stiffness compared to the one of the member being reinforced. In the figure 2, the strength-strain behaviour in tension of steel is compared with several commercial FRP products.

FRP material is characterized by an elastic behaviour with the elastic modulus E_f, the tensile (compressive) strength $\sigma_{f,u,t}$ ($\sigma_{f,u,c}$) and the Poisson coefficient ν_f. In this paper, three longitudinal and one transverse CFRP 530 (4x0.19 mm) sheets are placed around the outer perimeter of iron members; they have the following properties: E_f = 640 GPa, $\sigma_{f,u,t}$ = 2650 MPa and ν_f = 0.28. The compressive strength $\sigma_{f,u,c}$ is assumed equal to the tensile one. The thickness of FRP layer is assumed very small in comparison to the dimensions of the columns.

MEMBER IMPERFECTION

As for other metallic columns, cast iron columns possess an out-of straightness imperfection. In this paper, its amplitude is chosen equal to 1/1000 of the column length.

CROSS-SECTION IMPERFECTION

In circular hollow cast iron sections, the internal and external diameters are frequently eccentric, as shown in figure 3. The irregular wall thickness is the result of lifting forces, dislocations and/or deflections of the casting core used for producing the hole of the member during casting in the horizontal position. This geometrical eccentricity of the hole leads to an eccentricity (g) of the load with reference to the centroid of the cross-section. By examining a specimen extracted from the tested columns, values of the geometric parameters have been obtained: d_e = 126.5 mm, d_i = 94 mm, t_{min} = 14.5 mm, t_{max} = 18 mm, j = 1.75 mm and g = 2.16 mm. These ones have been assumed, for the simplicity, constant along the column in all the performed numerical simulations.

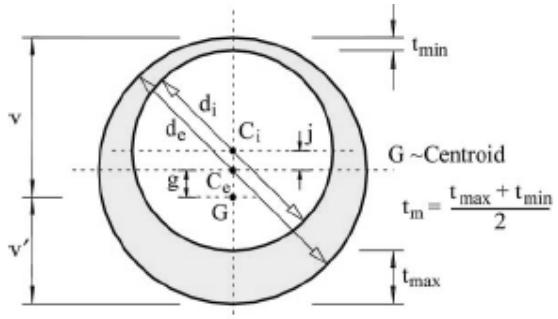

Figure 3: Cross-section imperfection in circular hollow cast iron columns

NUMERICAL MODEL

The response of iron elements under axial compression has been studied numerically with the homemade non-linear FEM software Finelg developed since three decades at Liège University. Beam elements with circular hollow sections are used to simulate the actual behaviour of FRP reinforced iron columns under axial compression forces; member out-of-straightness and section imperfections have been considered, as well as the anisotropy of iron in post elasticity and the contribution of the FRP sheets.

ANALYTICAL FORMULATION

An analytical formulation is proposed by Rondal and Rasmussen (Rondal et al. 2003) for the buckling resistance of iron columns under axial compression. Its extension to FRP reinforced iron is here contemplated. As iron is quite resistant in compression, but relatively weak in tension, two possible failure modes have to be successively considered (figure 4):

- failure by excess of compression on the thin side;
- failure by excess of tension on the thick side.

The location where failure occurs in the section (thin or thick side) results from the eccentricity g_{eq} between the centroid and the load introduction axis.

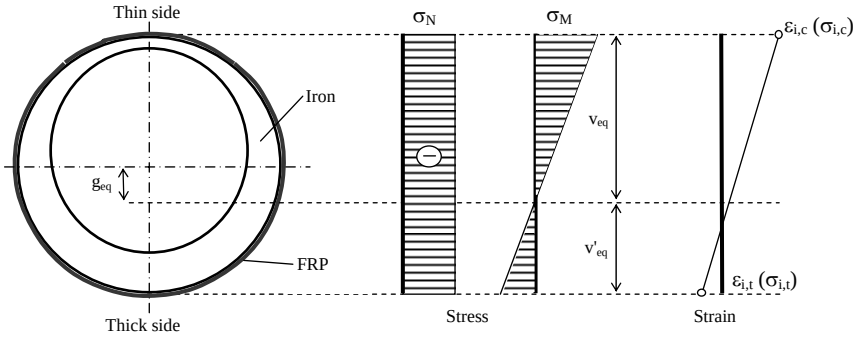

Figure 4: Strain and stress profile for FRP-iron composite section

Compression failure

The nominal buckling compressive stress $\sigma_{b,c}$ (N_u/A_{eq} with A_{eq} defined as $A_i + n_{eq}A_f$, and A_i, n_{eq} and A_f defined at the end of the paper), when the column reaches the buckling resistance (N_u), can be derived by the following formula:

$$\sigma_{b,c} = \chi_c \sigma_{i,0.2,c} \tag{2}$$

where $\sigma_{i,0.2,c}$ is the 0.2% proof stress of iron in compression and χ_c, the slenderness reduction factor calculated when the most stressed iron or FRP fibre (the farthest fibre) reaches its elastic strength ($\sigma_{i,0.2,c}$ or $\sigma_{f,u,c}$). In other way, the farthest fibre of the equivalent cross-section reaches a stress $\sigma_{i,c}$ corresponding to a strain $\varepsilon_{i,c}$, the latter being defined as the minimum of the two value $\varepsilon_{i,0.2,c}$ and $\varepsilon_{f,u,c}$, see figure 4. If f_c designates the ratio $\sigma_{i,c}/\sigma_{i,0.2,c}$, then χ_c can be calculated as follows:

$$\chi_c = \frac{f_c}{\varphi_c + \sqrt{\varphi_c^2 - f_c \overline{\lambda}^2}} \tag{3}$$

with:

$$\varphi_c = \frac{1}{2}(1 + \eta_c + f_c \overline{\lambda}^2) \tag{4}$$

where:

$$\overline{\lambda} = \frac{\lambda}{\lambda_e} \tag{5}$$

$$\lambda = \frac{L}{r_{eq}} \tag{6}$$

$$r_{eq} = \sqrt{\frac{I_{eq}}{A_{eq}}} \tag{7}$$

and:

$$\lambda_e = \pi \sqrt{\frac{E_i}{\sigma_{i,0.2,c}}} \tag{8}$$

The imperfection parameter η_c is given by:

$$\eta_c = \alpha \left[\left(\overline{\lambda} - \lambda_1 \right)^{\beta} - \lambda_0 \right] + g_{eq} A_{eq} \frac{v_{eq}}{I_{eq}} \tag{9}$$

(α, β, λ_0, λ_1), accounting for the column imperfection, depend on the material parameters n and $e = \sigma_{i,0.2,c} / E_i$. They can be evaluated by formulae proposed in Rasmussen et al. 2000. The parameter $g_{eq} A_{eq} v_{eq} / I_{eq}$ accounts for the cross-section imperfection.

Tension failure

Cast iron is relatively weak and brittle in tension; a column failure by excess of tension may be observed, as a result of the development of significant second-order bending moment in slender columns. The verification of the tension failure mode can be achieved through the following resistance formula:

$$\sigma_{b,t} = \chi_t \sigma_{i,0.2,c} \tag{10}$$

As in the previous paragraphs, χ_t should be calculated when the farthest iron or FRP fibre reaches its elastic strength in tension ($\sigma_{i,0.2,t}$ or $\sigma_{f,u,t}$). But in practice the FRP strength $\sigma_{f,u,t}$ is much higher than the iron one; so the tension failure takes place in the iron material. If f_t designates $\sigma_{i,0.2,t}/\sigma_{i,0.2,c}$, the slenderness reduction factor χ_t can be calculated through the following formula:

$$\chi_t = \frac{f_t}{\varphi_t + \sqrt{\varphi_t^2 + f_t \overline{\lambda}^2}} \tag{11}$$

where:

$$\varphi_t = \frac{1}{2}(-1 + \eta_t + f_t \overline{\lambda}^2) \tag{12}$$

and:

$$\eta_t = \alpha\left[\left(\overline{\lambda} - \lambda_1\right)^{\beta} - \lambda_0\right] + g_{eq} A_{eq} \frac{v'_{eq}}{I_{eq}} \tag{13}$$

$g_{eq} A_{eq} v'_{eq} / I_{eq}$ is the parameter accounting for the cross-section imperfection in case of tension failure mode.

APPLICATION TO IRON COLUMNS WITHOUT FRP

Results of the numerical simulations and of the application of the above described analytical model to iron columns without FRP are reported in figure 5, in the form of column buckling curves. "N_B" ($\overline{N}$) is the non-dimensional resistance:

$$\overline{N} = \frac{N_u}{\sigma_{i,0.2,c} A_i} \tag{14}$$

and "Lambda B_i" ($\overline{\lambda_i}$), the non-dimensional slenderness for iron columns without FRP in axial compression:

$$\overline{\lambda_i} = \frac{L}{\sqrt{\frac{I_i}{A_i}}} \frac{1}{\lambda_e} \tag{15}$$

, A_i and I_i are the area and the second moment inertia of the column sections.

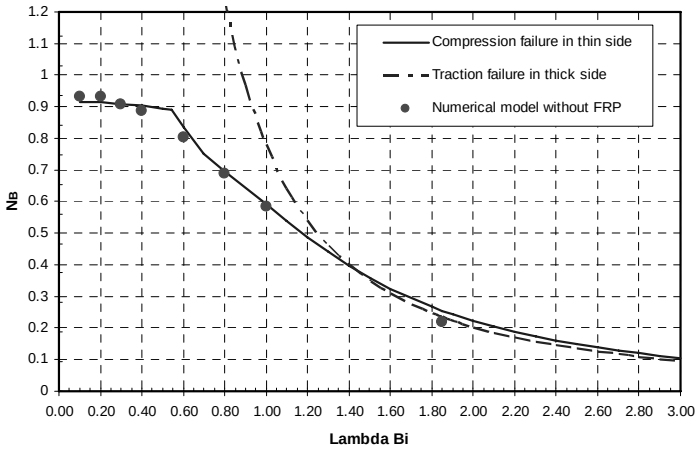

Figure 5: Axial compression buckling curves "$\overline{N}$ - $\overline{\lambda_i}$" for iron columns without FRP

The dashed curve presents analytically computed buckling resistances associated to a tension failure mode in the thick side and the continuous curve, associated to a compression failure in the thin side; the dots correspond to numerical simulations. The more the column is slender, the more it risks failing by tension mode.

The good agreement between numerical and analytical models, whatever the failure modes, indicates that the analytical proposal describes well the buckling resistance of iron columns. Anyway, the numerical and analytical models must still be validated by experimental tests.

APPLICATION TO IRON COLUMNS WITH FRP

In order to compare easily results carried out for iron columns respectively with and without FRP, all the buckling curves will be presented in a "N_B - Lambda B_i" format. "N_B" ($\overline{N}$) is the non-dimensional resistance defined by the formula (14) and "Lambda B_i" ($\overline{\lambda_i}$), the non-dimensional slenderness of corresponding columns without FRP defined by the formula (15).

Deformation capacity of FRP

For the studied iron material, the compressive strain at the 0.2% compressive proof stress $\varepsilon_{i,0.2,c}$ is equal to 0.626% and the tensile one $\varepsilon_{i,0.2,t}$, 0.085%. As mentioned previously, the strain $\varepsilon_{f,u,c}$ of longitudinal FRP in compression must be limited at a certain value because of the local buckling problem due to debonding effects. If the limit value 0.13%, much lower than $\varepsilon_{i,0.2,c}$ of iron, is used in the numerical simulations, results are those plotted in figure 6: the two dashed curves represent the analytical buckling resistances of iron columns without FRP, whereas the dots are numerical buckling resistances of iron columns with longitudinal FRP strips only.
It may be seen that longitudinal FRP strips, with a limited compressive strain associated to out-of-plane buckling effects, do not improve significantly the buckling resistance of iron columns. That is why transverse FRP strips should be applied in addition to longitudinal ones so as to avoid debonding effects.

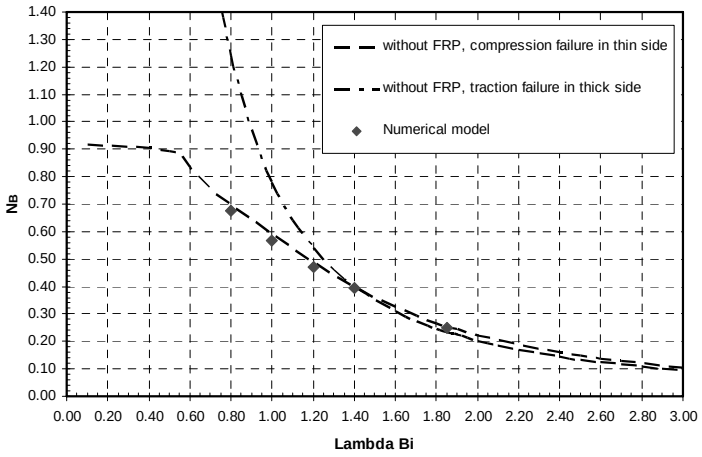

Figure 6: Axial compression buckling curve for iron columns with only longitudinal FRP

Buckling resistance of iron columns with FRP

Now, with the use of transverse FRP strips, the longitudinal FRP strips can reach the maximum strain $\varepsilon_{f,u,c}$ ($E_f/\sigma_{f,u,c}$) equal to 0.414%. By introducing this value in the numerical and analytical models, results shown in figure 7 are obtained: the two dashed curves represent analytical buckling resistances of iron columns without FRP, while the two continuous curves correspond to analytical buckling resistances of FRP reinforced columns; again the dots indicate numerical buckling resistances of iron columns with FRP.

The obtained numerical and analytical results are in good agreement for stocky or very slender columns, but not very optimal for the range of medium slenderness in which buckling resistance significantly depends on the initial member out-of-straightness or section imperfections. As the imperfection parameters (α, β, λ_0, λ_1) have been proposed for iron material, but not for the composite one composed of iron and FRP, new imperfection levels should be found so as to improve the proposed analytical formulation. Anyway, the actual analytical formulation gives safe results.

CONCLUSIONS

The following conclusions may be drawn from the numerical and analytical investigations on FRP reinforced iron columns under axial compression:

- FRP can be used to reinforce slender iron columns.

- In order to maximise the reinforcement, FRP used for longitudinal strips should be chosen such that its maximum compressive strain is at least equal to the compressive elastic strain of iron
- Transverse FRP strips should be used to avoid out-of-plane buckling effects in the longitudinal ones.
- The proposed analytical model can be used to predict the buckling resistance, but the accuracy of the model could be improved by defining an appropriate imperfection parameter (α, β, λ_0, λ_1) for FRP-iron composite columns. That may be one of the objectives for further developments.

The presented design method is based on the modern buckling curve approach, as for steel columns. It differs from the traditional methods used a century ago by the following aspects: (i) first the 0.2% proof stress is used as the upper bound, rather than the ultimate compressive strength, and (ii) secondly, explicit design equations are used to determine the tension failure strength rather than imposing a limit on the column slenderness. Experimental tests planned to be carried out soon at Liège University should allow to validate the proposed numerical and analytical models.

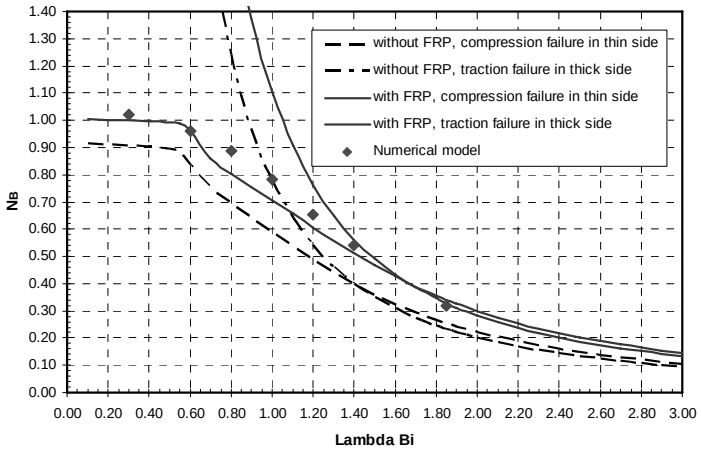

Figure 7: Axial compression buckling curves for iron columns with FRP not experiencing local buckling

REFERENCES

Bates, W. (1991), "Historical structural steelwork handbook", *The British constructional steelwork association*, ISBN 0 85073 015 5, 4th impression.

Blanchard, J., Bussell, M., Marsden, A. and Lewis, D. (1997). "Appraisal of existing ferrous metal structures", *Stahlbau 6*.

Bussell, M. (1997), "Appraisal of existing iron and steel structures", *SCI publication 138*, ISBN 1 85942 009 5.

Bussell, M.N. and Robinson, M.J. (1998). "Investigation, appraisal and reuse of a cast-iron structural frame", *Ordinary Meeting, The Structural Engineer*.

BUYUKOZTURK O. et al (2004). "Progress on understanding debonding problems in reinforced concrete and steel members strengthened using FRP composites", Construction and Building Materials 18 (2004) 9-19.

Fawzia, S. et al (2006). "Experimental and finite element analysis of a double strap joint between steel plates and normal modulus CFRP", *Composite Structure* 75 (2006) 156-162.

Fawzia, S. et al (2007). "Strengthening of circular hollow steel tubular sections using high modulus CFRP sheets", *Construction and Building Materials* 21 (2007) 839-845.

Fawzia, S. et al. "Bond characteristics between CFRP and steel plates in double strap joints", Department of Civil Engineering Monash University, Clayton, Victoria 3800, Australia.

Guerrieri, M.R., Di Lorenzo, G. and Landolfo, R. "Influence of atmospheric corrosion on the XIX century iron structures: assessment of damage for Umberto I Gallery in Naples".

Käpplein, R. (1991). "Assessment of the load bearing capacity of old cast iron columns", *Fourth International Colloquium on Structural Stability*, Istanbul.

Käpplein, R. (1997). “Untersuchung und Beurteilung alter Gubkonstruktionen”, *Stahlbau 6*.

Rasmussen, K.J.R. and Rondal, J. (2000). "Strength curves for aluminium alloy columns", *Engineering Structures* 23 (2000) 1505-1517.

Rondal, J. and Rasmussen, K.J.R. (2002). “Old industrial buildings: the cast-iron column problem”, *International Colloquium on Stability and Ductility of Steel Structures*, Akademiai Hiado, Budapest.

Rondal, J. and Rasmussen, K.J.R. (2003). “On the strength of cast iron columns”, *Research report N°R829*.

Rondal, J. and Rasmussen, K.J.R. (2005). “Design of cast iron columns with explicit calculation of tension fracture capacity”, *Eurosteel 2005 - 4th European conference on steel and composite structures*, Maastricht, the Netherlands.

Shaat, A. and Fam, A. (2006). "Axial loading tests on short and long hollow structural steel columns retrofitted using carbon fibre reinforced polymers", *J. Civ. Eng.* 33: 458-470.

Shaat, A. and Fam, A. (2007), "Fiber-Element model for slender HSS columns retrofitted with bonded high-modulus composites", *J. Struc. Eng.* ASCE.

Shaat, A. and Fam, A. (2007). "Finite element analysis of slender HSS columns strengthened with high modulus composites", *Steel and Composite Structures*, Vol 7, No 1 (2007) 19-34.

NOTATIONS

A_f	Cross-section area of FRP
A_i	Cross-section area of iron
d_e	Outer diameter
d_i	Inner diameter
n_{eq}	Equivalent coefficient of FRP modulus compared with the iron one (E_f/E_i)
A_{eq}	Equivalent cross-section area ($A_i + n_{eq}A_f$)
I_{eq}	Equivalent second moment of a composite cross-section ($I_i + n_{eq}I_f$)
I_i	Second moment of iron cross-section
I_f	Second moment of FRP cross-section
g_{eq}	Gravity centre of composite cross-section
v_{eq}	Distance of the farthest compressive fiber to g_{eq}
v'_{eq}	Distance of the extreme tensile fiber to g_{eq}
r_e	Outer rayon
r_i	Inner rayon
E_f	Elastic modulus of FRP
E_i	Elastic modulus of iron
L	Length of columns
N_u	Buckling resistance in compression
r	Gyration radius
t_{max}	Thickness of the thick side of iron cross-section
t_{min}	Thickness of the thin side of iron cross-section
$\sigma_{f,u,c}$	Compressive strength of FRP
$\varepsilon_{f,u,c}$	Compressive strain of FRP
$\sigma_{f,u,t}$	Tensile strength of FRP
$\varepsilon_{f,u,t}$	Tensile strain of FRP
$\sigma_{i,0.2,c}$	0.2% proof stress of iron in compression
$\varepsilon_{i,0.2,c}$	Strain at 0.2% proof stress of iron in compression
$\sigma_{i,0.2,t}$	0.2% proof stress of iron in tension
$\varepsilon_{i,0.2,t}$	Strain at 0.2% proof stress of iron in tension